< This part is filled by the editors (use jmoJournalTitle). >

Hemodynamics in the retinal vasculature during the progression of diabetic retinopathy

Francesco Calivá[1*], Georgios Leontidis[1*], Piotr Chudzik[1], Andrew Hunter[1], Luca Antiga[2], Bashir Al-Diri[1]

[1]*School of Computer Science, University of Lincoln, Lincoln, United Kingdom*, [2]*OROBIX srl, Bergamo, Italy*

Abstract

Purpose: Several studies have established, using various measurement modalities, that progression from diabetes to diabetic retinopathy is associated with changes in haemodynamics or measurable vascular geometry. In this study we take vessel measurements from standard fundus images, and estimate haemodynamic parameters (which are not directly observable) using a simple haemodynamic model. We show that there are statistically significant changes in some estimated haemodynamic parameters associated with the development of DR.
Methods: A longitudinal study of twenty-four subjects was conducted. For each subject four fundus images were used, taken annually during the three years before the appearance of DR and in the first year of DR. A venous and arterial vascular bifurcation, each of which consisted of a parent vessel and two child branches was extracted, and at the branching nodes a zero dimensional model estimated the fluid dynamic conditions in terms of volumetric blood flow, blood flow velocity, nodal pressure, wall shear stress and Reynolds number. These features were statisticlly analyzed using linear mixed models.
Results: A number of parameters, primarily venous, showed significant change with the development of DR, including early change two years before the onset of DR. A large proportion of overall variance is accounted for by individual patient differences, making progressive study essential.
Conclusion: This is the first paper to demonstrate that haemodynamic feature estimates extracted from standard fundus images are sensitive to progression from di-

Correspondence: Francesco Calivá.
E-mail: fcaliva@lincoln.ac.uk

[*] Francesco Calivá and Georgios Leontidis are co-first authors

abetes to DR. In our future work, we aim to test whether the variations in haemodynamic conditions are predictive of progression prior to the appearance of retinal lesions.

Keywords: Retinal microcirculation, Diabetic Retinopathy, Retinal trees, Retinal vascular geometry, Retinal biomarkers

1. Introduction

Diabetic retinopathy (DR) is characterized by lesions and vascular abnormalities, which include but are not limited to microaneurysms, haemorrhages, cotton wool spots, exudates (bright spots), venous beading, intraretinal microvascular abnormalities, neovascularization, loop and fibrous proliferation (Donnelly et al.[1], Leontidis et al.[2]). The World Health Organization (WHO) suggests that between 1980 and 2014, the prevalence of diabetes increased from 4.7% to 8.5%. In 2012, 1.5 million deaths were directly associated with diabetes and another 2.2 million deaths were linked to high blood glucose levels (WHO[3]). The early diagnosis of DR would allow clinicians to suggest patient-specific treatment plans for patients affected by diabetes, and ensure an efficient monitoring of the disease.

1.1 Retinal vascular geometry and haemodynamics

Haemodynamic factors such as perfusion pressure, vascular resistance, and blood viscosity together with the vascular geometry determine the distribution of blood flow to the retina (Harris et al.[12]), although the mechanisms linking haemodynamic alterations to systemic or ocular diseases are not completely understood yet (Caprioli et al.[17], Weinreb et al.[18]). Technologies such as *Retinal Vessel Analyzer* (Vilser et al.[13]), Doppler-based techniques (Nicolela et al.[14], Wang et al.[15]), and Retinal Function Imaging (Izhaky et al.[16]) allow non-invasive study of the retinal haemodynamics.

Several studies have (separately) investigated the effects of diabetes on the retinal vascular geometry and haemodynamics. Burgansky et al.[4] studied the effect of DR on the arterial blood flow velocity, which was found to be slower in patients with DR. Grunwald et al.[5] recruited a group of patients, which have been affected by diabetes for less than 4 years, and age-matched them with normal subjects. The total measured blood flow rate in the diabetic patients was significantly higher compared to the normal subjects. Leontidis et al.[6,7] observed significant changes in fractal dimension and arterial and venular widths. Kifley et al.[8] observed a relationship between the increase of DR's severity and the widening of retinal venular width. The Wisconsin epidemiological study showed that a correlation between the widening of retinal venulae and the progression of retinopathy exists (Klein et al.[9]). Yang et al.[10] observed only wider venular caliber in the presence of diabetic retinopathy.

1.2 Novelty of this study

In this paper we introduce a O-D model for the estimation of haemodynamic parameters from standard fundus images, and evaluate whether alteration of these estimated parameters is associated with the progression from diabetes to DR. This is potentially a more informative route to the detection of vascular disease than direct correlation from geometry measurements to disease, since the hypothesised cause of changes in vessel geometry is reaction to haemodynamic factors. Taking into account that the vascular geometry may be influenced by multiple factors including age, duration of diabetes, lifestyle, gender and phenotypic variation, the progression of the disease was investigated over a four-year period culminating in first diagnosis of DR, by analyzing fundus images from a cohort of twenty-four patients. The main contribution of this study is to establish that there are significant associations between the estimated haemodynamic features and the progression of the disease; to the best of the authors' knowledge, this has never been attempted before.

2. Methods & Results

A longitudinal study of twenty-four patients was conducted. Ninety-six fundus photographs (FP) (1700$\times$1700 pixels) were selected from the diabetic screening service of Pilgrim Hospital in Boston, UK. For each patient, four photographs were captured annually during the three years before DR and in the first year of DR.

2.1 Retinal blood flow mechanics

Blood vessels were segmented out by using the Ribbon of Twins (RoT) method (Al-Diri et al.[19]). The RoT technique is an active contour method that uses morphological filters to identify the centerline of a vessel, and exhibits excellent performance in extracting edges. In each selected fundus image, one arterial and one venous bifurcation (see Fig. 1a) were reconstructed using a semi-supervised tool (Calivá et al.[20]); a bifurcation consists of three vessel segments, the parent and its two children. For each patient the same venous and arterial bifurcations were selected throughout the four-year period, making analysis of changes meaningful.

2.2 0-D vascular model

A zero-dimensional model was designed to simulate the fluid dynamics within the network. As the diameter of the vessels was below $200\mu m$, the haemodynamics would be in the microcirculation regime (Wong et al.[21], Pournaras et al.[11]), where Fahraeus and Fahraeus-Lindqvist effects, and plasma skimming, are crucial in determining the distribution of the hematocrit and the blood flow velocity profile (Pries et al.[22,23]). However, for simplicity our model treats the blood as a Newtonian fluid (Aletti et al.[24]).The flow of blood was modelled as 0-D, and thus the mean blood flow velocity was used. The blood flow was assumed to follow Hagen-Poiseuille's law

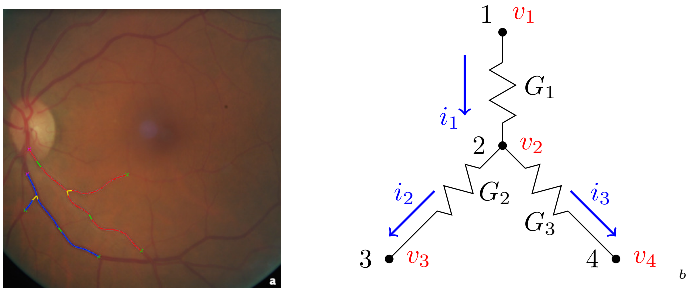

Fig. 1. **Left:** An arterial (red) and venous (blue) tree. Bifurcations are colored yellow. The green dashes represent the connection between the segments in which a blood vessel is split by the segmentation algorithm. **Right:** A lumped electric circuit. Nodes are denoted by the numbers $1, 2, 3$ and 4; nodal voltages by v_i, with $i = 1, \ldots, 4$; currents by i_k, with $k = 1, \ldots, 3$; conductances by G_k, with $k = 1, \ldots, 3$. The blue arrows represent the current flow direction.

(H-P). H-P flow describes the relationship between the pressure drop (ΔP) and the blood flow through a tube ($\Delta P = R_i \cdot Q_i$), under the assumptions of a stiff, straight and uniform tube; a Newtonian fluid; a circular cross section; a laminar, steady (i.e. not pulsatile) flow with null velocity at the wall (no slip condition). $R_i = \frac{8\mu L_i}{\pi r_i^4}$ is the resistance that the blood encounters when flowing in the i^{-th} tube of radius r_i and length L_i, with $\mu = 0.04P$ the blood viscosity; $G_i = \frac{\pi r_i^4}{8\mu L_i}$ is the conductance of the vessel. The retinal network was studied with an electrical lumped elements model. The conservation of mass was assumed at the branching nodes. Hence, the inflow of blood at the inlet matched the outflow from the bifurcation. Similar to Kirchhoff's conservation law of electric current at each node, for the j^{-th} branching point, the relationship $\sum_{k=p,d_1,d_2} Q_{j,k} = 0$ holds, where p, d_1, d_2 refers to the parent branch and the two child branches of the bifurcation respectively (Causin et al.[25]). By combining H-P's law and the segment's conductance term, an explicit equation for Q was obtained ($\Delta Q_{jk} = G_{jk} \cdot \Delta P_{jk}$) in which the subscripts j and k refers to the node of the circuit (e.g. see Fig. 1b). For the circuit in Fig. 1b, the pressure value at each node was computed by applying the conservation law, and solving the system of linear equations $Q_{jk} = \Delta P_{jk} G_{j,k}$. Fig. 1b shows an example of a circuit, which represents a tree displayed in Fig. 1a. In this circuit, by applying Kirchhoff's law at each node of the system, Eq. 1 was obtained and by its solution the pressure values at each node of the circuit could be then computed.

$$\begin{bmatrix} 1 & 0 & 0 & 0 \\ G_1 & -(G_1 + G_2 + G_3) & G_3 & 0 \\ 0 & 0 & 1 & 0 \\ 0 & 0 & 0 & 1 \end{bmatrix} \cdot \begin{bmatrix} P_1 \\ P_2 \\ P_3 \\ P_6 \end{bmatrix} = \begin{bmatrix} P_{in} \\ 0 \\ P_{out3} \\ P_{out6} \end{bmatrix} \tag{1}$$

2.2.1 Boundary conditions (BCs)

The fluid dynamic conditions in the arterial and venular trees, which included one bifurcation, were computed. Two experiments were carried out. In the first, BCs were set up in terms of pressure, in the second in terms of blood flow.

Pressure boundary conditions At the inlet (parent of the bifurcation), a pressure value of 40 mmHg was specified. This choice reflects the hydrostatic and frictional pressure losses from the aorta to the Central Retinal Artery (CRA). At the outlet (children of the bifurcation), a pressure slightly higher than 15 mmHg, which is equivalent to the intraocular pressure (IOP) in normal condition, was enforced to prevent vessels collapse.

Flow boundary conditions At the inlet, Q was computed as $Q_i(r_i) = \pi r_i^2 \overline{v_i}$. For the arterial trees, the enforced Q was computed based on a mean velocity blood flow ($\overline{v} = 6.4cm/s$), measured in the CRA by Fuchsjäger et al.[26] by using Color Doppler Imaging, and a CRA's diameter of 166 μm suggested by Pemp et al.[27]. In the venous trees, the literature reports values of blood flow velocity and diameter in which the central retinal vein (CRV) can vary (Kaiser et al.[28], Pemp et al.[27]). The mean velocity blood flow used in this work was $\overline{v} = 3.6cm/s$, and CRV's diameter $D = 210\mu m$. At the outlet, the blood flow was enforced by assuming that at the bifurcation point the blood flow velocity is constant. Therefore, with regard to the equation which expresses the relationship between vessel's caliber, blood flow rate and blood flow velocity, in each of the branches (i.e. parent and children), Q depends only on the vessels' caliber squared and was computed as $Q_j = Q_{in} \cdot \frac{r_j^2}{\sum_{k \in Outlet} r_k^2}$.

2.3 Hemodynamic parameter estimates

The nodal pressure (*P*) was estimated by solving the system in Eq. 1. In each vessel, four parameters were estimated. The flow rate (*Q*) was computed by solving Poiseuille's law equation. The wall shear stress (*WSS*) was computed in each i^{-th} vessel as $WSS_i = \frac{32\mu Q_i}{\pi D_i^3}$. The blood flow velocity (*v*) was computed in each vessel, by rearranging and solving the equation, which expressed the relationship between $\overline{v_i}$, Q and r. The Reynolds number (*Re*) was computed as $Re = \frac{\overline{v} D \rho}{\mu}$, where $\rho = 1.060 g/mL$ was the dynamic viscosity of the blood.

2.4 Statistical analysis

The statistical analysis relates the five estimated haemodynamic features, both venous and arterial, to the year of measurement (i.e. progression towards disease), while accounting for individual differences between patients. The analysis was performed using linear mixed effects models (LMM) (Bates[29]), in which fixed and random effects combine linearly with an error term to determine a response variable. LMMs are similar to the Analysis of Variance (ANOVA) test, but they are considerably more generalized, supporting post-hoc analysis and utilizing additional evaluation metrics, as can be seen in the model comparison part that follows (Krueger et al.[30]).The LMM captures individual differences by estimating a different random intercept for each subject.

A "full" LMM was constructed for each feature, with the feature as the response variable, the year of measurement as the (independent) variable of fixed effects and the subject identity as the (independent) variable of random effects. A second, "restricted" model was also constructed for each feature, with the subject identity as the sole independent (random effects) variable.

The models were used to investigate the relationship of the year of measurement to the features as follows. First, the full models were fitted using restricted maximum likelihood (REML) and the Welch–Satterthwaite estimation of p-values based on degrees of freedom (Satterthwaite[32]) calculated. Second, both the full and restricted models were fitted using Maximum Likelihood (ML), p-values calculated from the likelihood ratio between the predictions of the two models, and the Akaike information criteria (AICs) calculated for both models. The restricted models were used to calculate the intra-class correlation (ICC), which describes the proportion of the total variance that can be explained by the individual patient identity. Post-hoc comparisons were made to investigate the relationship between the year of measurement and the statistically significant features; a Tukey-test was used to identify which year group means differed (Tukey[33]). The analyses were carried out in a balanced design. Table 1 lists the results for all the estimated parameters with significant results ($p < 0.05$). The lower AIC values for the "full" models indicate superior performance to the "restricted" models, showing that the year of measurement is related to the reported features; the two p-values are alternative methods that indicate the statistical significance of this relationship. All five venous parameters show significant results, with stronger effects in the child vessels, and wall shear stress and velocity particularly affected. In the arteries, effects are seen only in the volumetric blood flow and Reynold's number parameters in the child vessels. The ICC values show that, particularly in the venous analysis, there is a high level of individual patient variation, so that the strategy of including the patient identity as a random effects factor in the context of a longitudinal study was crucial to the success of the model.

Table 2 presents the post-hoc analysis of the features, listing the year to year comparisons where a significant difference was detected, with associated p-values. For the venous features with the strongest effects (e.g. *WSS*, *v* and *Re* in the first child vessel) there is a consistent pattern that the most significant effects are between year 3 and the other years: year 2, year 0 (DR onset) and year 1 in that order. The dip in significance in year one suggests there may be a complex development of the haemodynamics features. Given the difference in methods and modalities a direct comparison could not be made with other studies, although we note that elsewhere (e.g. Bursell et al.[34], Grunwald et al.[35], Feke et al.[36]) contradictory findings on blood

Table 1. The haemodynamic features showing statistically significant relationship to year of measurement. Lower AIC values for "full" models indicate that the measurement year is significant; the two alternative p-value estimates confirm the significance of this difference. The ICC illustrates the proportion of variance accounted for by other differences between individual patients.

Features	AIC[a]	p-(s)[b]	p-(LR)[c]	ICC
Veins_WSS_Parent	550.7/554.3	0.02	0.02	0.942
Veins_WSS_Child1	472.2/484.8	<0.000	<0.000	0.917
Veins_WSS_Child2	490.7/501.2	0.001	<0.000	0.901
Veins_Q_Child1	201.4/204.1	0.05	0.034	0.955
Veins_Q_Child2	201.4/204	0.04	0.033	0.915
Veins_v_Parent	335.5/339.2	0.024	0.02	0.833
Veins_v_Child1	231.9/247.2	<0.000	<0.000	0.896
Veins_v_Child2	247.5/256.1	0.003	0.002	0.915
Veins_Re_Parent	693.4/696.8	0.027	0.024	0.922
Veins_Re_Child1	593.9/610.4	<0.000	<0.000	0.892
Veins_Re_Child2	608.3/611	0.04	0.034	0.944
Veins_Pressure	444.3/448.2	0.02	0.017	0.833
Arteries_Q_Child1	106.2/111.5	0.012	0.01	0.398
Arteries_Q_Child2	105.1/110.4	0.011	0.009	0.399
Arteries_Re_Child2	800.1/804.5	0.017	0.015	0.622

[a] Full/restricted. [b] P-value (Satterthwaite approximation). [c] P-value (likelihood ratio).

flow rates in normal and diabetic patients have been reported. The significant difference in year 3 to year 2 is particularly interesting, as it is suggestive of the potential for early detection of the onset of DR. In the arterial network, the smaller number of significant features are most consistently affected between year 3 and year 1.

3. Conclusions and future perspectives

In this paper, a number of retinal haemodynamic parameters (nodal pressure, volumetric blood flow, wall shear stress, blood flow velocity and Reynolds number) were estimated using a 0-D model, using measurements extracted from selected vessel bifurcations on fundus images. The estimated parameters were analyzed over a period of three years of progression from diabetes to DR, within a group of twenty-four subjects. The results indicate that there are significant alterations to haemodynamic parameter estimates associated with detectable changes to vessel geometry, particularly in the venular network. These are particularly pronounced between the earliest year studied (three years before DR onset) and subsequent years.

In future work, we will utilize a larger data set to verify these findings, include a

Table 2. Post-hoc analysis of the haemodynamic features, showing significant year to year differences. Differences from year 3 to other years predominate.

Features	Significant Hypotheses	P-values
Veins_WSS_Parent	Year3-Year2	0.015
Veins_WSS_Child1	Year3-Year2	0.002
	Year3-Year1	0.019
	Year3-DR	<0.000
Veins_WSS_Child2	Year3-Year2	<0.000
	Year3-Year1	0.009
	Year3-DR	0.003
Veins_Q_Child1	Year3-Year2	0.049
	Year2-DR	0.048
Veins_Q_Child2	Year3-Year2	0.049
	Year3-DR	0.049
Veins_v_Parent	Year3-Year2	0.015
Veins_v_Child1	Year3-Year2	0.001
	Year3-Year1	0.008
	Year3-DR	0.001
Veins_v_Child2	Year3-Year2	0.02
	Year3-Year1	0.005
	Year3-DR	0.002
Veins_Re_Parent	Year3-Year2	0.018
Veins_Re_Child1	Year3-Year2	<0.000
	Year3-Year1	0.009
	Year3-DR	<0.000
Veins_Re_Child2	Year3-DR	0.017
Veins_Pressure	Year2-Year1	0.013
	Year3-DR	0.024
Arteries_Q_Child1	Year3-Year1	0.006
Arteries_Q_Child2	Year3-Year1	0.006
Arteries_Re_Child2	Year3-Year2	0.035
	Year3-Year1	0.024

control sample to allow a full retrospective study, further investigate the evolution of the haemodynamic features during disease progression, and extend the analysis to full vascular trees that include multiple bifurcations. We will also validate the 0-D model predictions on functional images that include direct measurement of haemodynamic features in addition to the standard fundus appearance. Finally, we will develop diagnostic models to predict DR onset from estimated haemodynamic features.

Acknowledgements

This research was made possible by a Marie Curie grant from the European Commission in the framework of the REVAMMAD ITN (Initial Training Research network), Project number 316990. The authors would also like to thank Mr P. Hopkins, United Lincolnshire Hospitals NHS Trust, Pilgrim Hospital, Diabetic Eye Screening Programme, Boston, United Kingdom, for letting us extract the fundus images.

References

1. Donnelly, Richard and Horton, Edward. Vascular complications of diabetes: current issues in pathogenesis and treatment. John Wiley & Sons, 2008;
2. Leontidis, Georgios and Al-Diri, Bashir and Hunter, Andrew. Diabetic retinopathy: current and future methods for early screening from a retinal hemodynamic and geometric approach. Expert Review of Ophthalmology, 2014;9(5): 431–442.
3. WHO. Global report on diabetes. 2016;
4. Burgansky-Eliash Z, Nelson DA, Bar-Tal OP, Lowenstein A, Grinvald A, Barak A. Reduced retinal blood flow velocity in diabetic retinopathy. Retina, 2010;30(5): 765–773.
5. Grunwald JE, Maguire AM, Dupont J. Retinal hemodynamics in retinitis pigmentosa. American journal of ophthalmology, 1996;122(4): 502–508.
6. Leontidis, Georgios and Al-Diri, Bashir and Wigdahl, Jeffrey and Hunter, Andrew. Evaluation of geometric features as biomarkers of diabetic retinopathy for characterizing the retinal vascular changes during the progression of diabetes. 2015 37th Annual International Conference of the IEEE Engineering in Medicine and Biology Society (EMBC). IEEE. 2015; 5255–5259.
7. Leontidis, Georgios and Al-Diri, Bashir and Hunter, Andrew. Summarising the retinal vascular calibres in healthy, diabetic and diabetic retinopathy eyes. Computers in biology and medicine, 2016;72, 65–74.
8. Kifley, Annette and Wang, Jie Jin and Cugati, Sudha and Wong, Tien Y and Mitchell, Paul. Retinal vascular caliber, diabetes, and retinopathy. American journal of ophthalmology, 2007;143(6): 1024–1026.
9. Klein, Ronald and Klein, Barbara EK and Moss, Scot E and Davis, Matthew D and DeMets, David L. The Wisconsin Epidemiologic Study of Diabetic Retinopathy: III. Prevalence and risk of diabetic retinopathy when age at diagnosis is 30 or more years. Archives of ophthalmology, 1984;102(4): 527–532.
10. Yang, Xiufen and Deng, Yu and Gu, Hong and Ren, Xuetao and Lim, Apiradee and Snellingen, Torkel and Liu, Xipu and Wang, Ningli and Pak, Jeong Won and Liu, Ningpu and others. Relationship of retinal vascular calibre and diabetic retinopathy in Chinese patients with type 2 diabetes mellitus: the Desheng Diabetic Eye Study. British Journal of Ophthalmology, 2016;
11. Pournaras, Constantin J and Rungger-Brändle, Elisabeth and Riva, Charles E and Hardarson, Sveinn H and Stefansson, Einar. Regulation of retinal blood flow in health and disease. Progress in retinal and eye research, 2008;27(3): 284–330.
12. Harris, Alon. Atlas of ocular blood flow: vascular anatomy, pathophysiology, and metabolism. Butterworth-Heinemann Medical, 2003;
13. Vilser, Walthard and Nagel, Edgar and Lanzl, Ines. Retinal vessel analysis-new possibilities. Biomedizinische Technik/Biomedical Engineering, 2002;47(s1b): 682–685.
14. Nicolela, Marcelo T and Hnik, Peter and Drance, Stephen M. Scanning laser Doppler flowmeter study of retinal and optic disk blood flow in glaucomatous patients. American journal of ophthalmology, 1996;122(6): 775–783.
15. Wang, Yimin and Lu, Ake and Gil-Flamer, John and Tan, Ou and Izatt, Joseph A and Huang, David. Measurement of total blood flow in the normal human retina using Doppler Fourier-domain optical coherence tomography. British Journal of Ophthalmology, 2009;93(5): 634–637.

16. Izhaky, D., Nelson, D. A., Burgansky-Eliash, Z., and Grinvald, A. Functional imaging using the retinal function imager: direct imaging of blood velocity, achieving fluorescein angiography-like images without any contrast agent, qualitative oximetry, and functional metabolic signals. Japanese journal of ophthalmology, 2009;53(4): 345–351.
17. Caprioli, Joseph and Coleman, Anne L and others. Blood pressure, perfusion pressure, and glaucoma. American journal of ophthalmology, 2010;145(5): 704–712.
18. Weinreb, Robert N and Harris, Alon. Ocular blood flow in glaucoma. 2009,6.
19. Al-Diri, Bashir and Hunter, Andrew and Steel, David. An active contour model for segmenting and measuring retinal vessels. IEEE Transactions on Medical imaging, 2009;28(9): 1488–1497.
20. Calivá, Francesco and Aletti, Matteo and Al-Diri, Bashir and Hunter, Andrew. A new tool to connect blood vessels in fundus retinal images. 37th Annual International Conference of the IEEE Engineering in Medicine and Biology Society (EMBC), 2015; 4343–4346.
21. Wong, T. Y., Klein, R., Klein, B. E., Meuer, S. M., and Hubbard, L. D. Retinal vessel diameters and their associations with age and blood pressure. Investigative ophthalmology and visual science, 2003;44(11): 4644–4650.
22. Pries, AR and Neuhaus, D and Gaehtgens, P. Blood viscosity in tube flow: dependence on diameter and hematocrit. American Journal of Physiology-Heart and Circulatory Physiology, 1992;263(6): H1770–H1778.
23. Pries, AR and Ley, K and Claassen, M and Gaehtgens, P. Red cell distribution at microvascular bifurcations. Microvascular research, 1989;38(1): 81–101.
24. Aletti, Matteo and Gerbeau, Jean-Frédéric and Lombardi, Damiano. Modeling autoregulation in three-dimensional simulations of retinal hemodynamics. Journal for Modeling in Ophthalmology, 2015;1.
25. Causin, P., Guidoboni, G., Malgaroli, F., Sacco, R., and Harris, A. Blood flow mechanics and oxygen transport and delivery in the retinal microcirculation: multiscale mathematical modeling and numerical simulation. Biomechanics and modeling in mechanobiology, 2016;15(3): 525–542.
26. Fuchsjäger-Mayrl, Gabriele and Polak, Kaija and Luksch, Alexandra and Polska, Elzbieta and Dorner, Guido T and Rainer, Georg and Eichler, Hans-Georg and Schmetterer, Leopold. Retinal blood flow and systemic blood pressure in healthy young subjects. Graefe's archive for clinical and experimental ophthalmology, 2001;239(9): 673–677.
27. Pemp, Berthold and Cherecheanu, Alina-Popa and Garhofer, Gerhard and Schmetterer, Leopold. Calculation of central retinal artery diameters from non-invasive ocular haemodynamic measurements in type 1 diabetes patients. Acta ophthalmologica, 2015;91(5): e348–e352.
28. Kaiser, Hedwig J and Schoetzau, Andreas and Flammer, Josef. Blood flow velocity in the extraocular vessels in chronic smokers. British journal of ophthalmology, 1997;81(2): 133–135.
29. Bates, Douglas. Computational methods for mixed models. LME4: Mixed-Effects Modeling with R, 2014; 99–118.
30. Krueger C, Tian L. A comparison of the general linear mixed model and repeated measures ANOVA using a dataset with multiple missing data points. Biological research for nursing, 2004;6(2): 151–157.
31. Akaike, Hirotogu. Information theory and an extension of the maximum likelihood principle. Selected Papers of Hirotugu Akaike. Springer, 1998; 199–213.
32. Satterthwaite, Franklin E. An approximate distribution of estimates of variance components. Biometrics bulletin, 1946;2(6): 110–114.
33. Tukey, John W. Comparing individual means in the analysis of variance. Biometrics, 1949; 99–114.
34. Bursell, Sven-Erik and Clermont, Allen C and Kinsley, Brendan T and Simonson, Donald C and Aiello, Lloyd M and Wolpert, Howard A. Retinal blood flow changes in patients with insulin-dependent diabetes mellitus and no diabetic retinopathy. Investigative ophthalmology & visual science, 1996;37(5): 886–897.
35. Grunwald, Juan E and DuPont, Joan and Riva, Charles E. Retinal haemodynamics in patients with early diabetes mellitus. British journal of ophthalmology, 1996;80(4): 327–331.

36. Feke, GT and Buzney, Sheldon M and Ogasawara, Hironobu and Fujio, Naoki and Goger, Douglas G and Spack, Norman P and Gabbay, Kenneth H. Retinal circulatory abnormalities in type 1 diabetes. Investigative ophthalmology & visual science, 1994;35(7): 2968–2975.